GEAR FATIGUE CRACK DIAGNOSIS BY VIBRATION ANALYSIS USING EMBEDDED MODELING

C. James Li and Hyungdae Lee

Dept. of Mechanical Engineering, Aeronautical Engineering & Mechanics
Rensselaer Polytechnic Institute
110 8th St., Troy, NY 12180
E-mail: lic3@rpi.edu

Abstract: This paper describes an embedded modeling methodology for identifying gear meshing stiffness from measured gear angular displacement or transmission error. An embedded model integrating a physical based model of the gearbox and a parametric representation, in the form of truncated Fourier series, of meshing stiffness is established. A solution method is then used to find the meshing stiffness that minimizes the discrepancy between model output and the measured output. Both simulation and experimental studies were conducted to evaluate if identified tooth meshing stiffness can reveal a tooth crack more effectively.

Key words: Crack; Embedded model; Gear diagnosis; Meshing stiffness; Torsional vibration; Transmission error.

INTRODUCTION

Figure 1 shows a dynamic model of a single-stage gearbox where θ represents angular displacement, I represents inertia, T represents torque, and k_m represents meshing stiffness between the two gears. Even if the gears are perfect, the meshing stiffness varies periodically as the number of teeth in contact and the contact point change. This non-constant meshing stiffness becomes a parametric excitation for gear vibration during gear rotation. Localized gear faults such as cracked or fractured teeth, that affect only a few teeth, introduce variations in meshing stiffness which, in turn, increase amplitude and phase modulations in gear vibrations.

To detect and assess tooth crack, existing gear fault diagnostic algorithms accentuate or extract magnitude and/or phase modulations from gear vibrations. Dalpiaz et al. [1] gave references for a number of early and modern gear diagnostic algorithms and Choy et al. [2] gave references on Wigner-Ville Distribution (WVD) and some statistical based methods including FM4, NA4 and NB4.

There are limitations for vibration based gear diagnostic methods. Vibrations are secondary effects in the sense that they are dynamic responses of a gearbox excited by meshing stiffness and other excitations. The effect of irregular meshing stiffness

associated with a cracked tooth is filtered by the gearbox dynamics and contaminated by other vibrations. Even when a cracked tooth is revealed by detectable amplitude/phase modulations, there is no straightforward relationship between the modulation amplitude and the crack size which is necessary for severity assessment and residual life prognosis.

In order to alleviate these limitations, this study has developed a method to identify meshing stiffness from measured gear vibration.

PROPOSED METHOD

The goal of this study is to establish the utility of embedded modeling method [3] to identify the meshing stiffness which is more directly related to the fault than vibration. A summary of the embedded modeling method is provided below.

Embedded modeling method: Let's say that the dynamics of a real system is described as

$$\begin{aligned} \dot{x} &= F(x, f) \\ s &= h(x) \end{aligned} \tag{1}$$

where x is the system state vector, f is the forcing function, s, also a vector, stands for system physical variables that are measured by transducers, h stands for the function relating the state and the measurable, s. It is also assumed that x, and s are n, and m dimensional, respectively. Let's further assume that the model of the system takes the following form

$$\begin{aligned} \dot{\hat{x}} &= \hat{F}(\hat{x}, f; \omega) \\ \hat{s} &= h(\hat{x}) \end{aligned} \tag{2}$$

where the circumflex stands for approximation, ω (p-dimensional) stands for the vector of model parameters that, at least, is partially unknown. Note that h is assumed to be known here to simplify the discussion.

One can show that model output $\hat{s}$ will approach the real system output, s if $\hat{F}$ approaches F provided the initial error is small. Therefore, it is natural to find the $\hat{F}$ that can minimize the difference between system and model outputs, i.e.,

$$\begin{aligned} E &= \frac{1}{2}\int_{t_0}^{t_f} e^T e dt \ (continuous) \quad or \\ E &= \frac{1}{2}\sum_{i=1}^{M} e_i^T e_i \ (discrete) \end{aligned} \tag{3}$$

where $e = s - \hat{s}$, and t_0 and t_f define the interval. Equation (3) is the so-called objective function.

Using nonlinear programming, Equation (3) can be minimized by an iterative procedure starting from an initial guess

$$\omega^{k+1} = \omega^k - \alpha R^k g^k \tag{4}$$

where g^k is the gradient of E at ω^k, R^k is a positive-definite square matrix and α defines the step size. The product of g^k and R^k gives the search direction. Using different R matrix yields different gradient-based updating schemes such as steepest descend and Newton's method with different efficiency, robustness and computation cost. This study used Levenberg-Marquardt method for its robustness.

To obtain the gradient one takes derivative of E with respect to ω which yields

$$g = \sum_{i=1}^{M} e_i^T \frac{\partial e_i}{\partial \omega} = -\sum_{i=1}^{M} \left(\frac{\partial \hat{s}_i}{\partial \omega} \right)^T (s_i - \hat{s}_i) \tag{5}$$

Note from above equation that gradient g is calculated from e and an $m \times p$ Jacobian matrix that contains the partial derivative of $\hat{s}$ with respect to ω. The Jacobian is denoted as J hereinafter. Taking derivative of $\hat{s}$ with respect to ω yields J as

$$J = \frac{\partial \hat{s}}{\partial \omega} = \left(\frac{dh}{d\hat{x}} \right)^T \frac{\partial \hat{x}}{\partial \omega} \tag{6}$$

However, the partial derivative of $\hat{x}$ with respect to ω is not readily available. Let's take partial derivative of the model or Eq. (2) with respect to ω to obtain the so-called sensitivity equation

$$\begin{aligned} &d\left(\frac{\partial \hat{x}}{\partial \omega} \right) / dt = \frac{\partial \hat{F}}{\partial \hat{x}} \frac{\partial \hat{x}}{\partial \omega} + \frac{\partial \hat{F}}{\partial \omega} or \\ &\dot{\xi} = \hat{F}_x' \xi + \hat{F}_\omega' \end{aligned} \tag{7}$$

where $\xi = \partial \hat{x} / \partial \omega$; $\hat{F}_x'$ and $\hat{F}_\omega'$ are the partial derivatives of $\hat{F}$ with respect to x and ω, respectively. Solution of Eq. (7) is the needed $\frac{\partial \hat{x}}{\partial \omega}$ which has an initial value as a zero matrix because the initial condition, $\hat{x}(t_0) = \hat{x}_0$, does not depend on the parameters of the model.

Formulating an embedded model for a gearbox : The model of a simple spur-gear transmission can be represented by a collection of masses, springs, and dampers as in

Figure 2 [4].

The non-linear equation of motion can be written as:

$$
\begin{aligned}
&J_M\ddot{\theta}_M + C_{s1}(\dot{\theta}_M - \dot{\theta}_1) + K_{s1}(\theta_M - \theta_1) = T_M \\
&J_1\ddot{\theta}_1 + C_{s1}(\dot{\theta}_1 - \dot{\theta}_M) + K_{s1}(\theta_1 - \theta_M) + C_g(t)(R_{b1}(R_{b1}\dot{\theta}_1 - R_{b2}\dot{\theta}_2)) + K_g(t)(R_{b1}(R_{b1}\theta_1 - R_{b2}\theta_2)) = T_{f1}(t) \\
&J_2\ddot{\theta}_2 + C_{s2}(\dot{\theta}_2 - \dot{\theta}_L) + K_{s2}(\theta_2 - \theta_L) + C_g(t)(R_{b2}(R_{b2}\dot{\theta}_2 - R_{b1}\dot{\theta}_1)) + K_g(t)(R_{b2}(R_{b2}\theta_2 - R_{b1}\theta_1)) = T_{f2}(t) \\
&J_L\ddot{\theta}_L + C_{s2}(\dot{\theta}_L - \dot{\theta}_2) + K_{s2}(\theta_L - \theta_2) = -T_L
\end{aligned}
\tag{8}
$$

where θ_M, θ_1, θ_2, and θ_L represent the rotations of the motor, the pinion and the gear, and the load; J_M, J_1, J_2, and J_L represent the mass moments of inertia; C_{s1}, C_{s2}, and C_g are damping coefficients of the shafts and the gear mesh; K_{s1}, K_{s2}, and K_g are stiffness of the shafts and the gear mesh; T_M, T_L, $T_{f1}(t)$, and $T_{f2}(t)$ are motor and load torques and frictional torques on the gears; R_{b1} and R_{b2} are base circle radii of the gears.

The meshing stiffness, i.e., K_g is assumed to be periodic. For a good gear that has regularly-spaced identical teeth, the meshing stiffness is largely repeated from one tooth to the next. In this case, a truncated Fourier series with a fundamental frequency of tooth meshing is used to represent K_g. (Note that Eq. (9) is formulated as a function of time. While it is more accurate for it to be a function of angular position, it is more convenient to have it as a function of time along which the gearbox dynamics evolves.)

$$
K_g(t) = \frac{a_0}{2} + \sum_{n=1}^{N}\left(a_n \cos(2\pi n f_m t) + b_n \sin(2\pi n f_m t)\right) \tag{9}
$$

where N is the number of harmonics included.

On the other hand, a faulty tooth gives a meshing pattern that is repeated only once a revolution. Therefore, a Fourier series with a fundamental frequency as the rotation frequency is more suitable.

$$
K_g(t) = (1 + \sum_{k=1}^{K}[c_k \cos(2\pi k f_s t) + d_k \sin(2\pi k f_s t)])K_g(t) \tag{10}
$$

where K is the number of harmonics considered. Equation (9) can be considered as a special case of Eq. (10) which can be used for both good and faulty gears. However, to cover the same number of meshing harmonics, Eq. (10) uses more terms than Eq. (9). This means more unknowns and therefore higher computational cost.

The damping, C_g, is assumed to be a function of the meshing stiffness

$$
C_g(t) = 2\zeta\sqrt{K_g(t)R_{b1}{}^2R_{b2}{}^2J_1J_2/(R_{b1}{}^2J_1 + R_{b2}{}^2J_2)} \tag{11}
$$

where ζ is the damping ratio [4].

To identify gear meshing stiffness from gear vibration, one takes the gearbox model, i.e., equations (8) – (11), and solves for Fourier coefficients a_i and b_i or c_i and d_i in the way ω_i is solved as described in the last section.

SIMULATION STUDY

A gearbox dynamic simulator, DANST (Dynamic Analysis of Spur Gear Transmissions) was extended to simulate a good gearbox and another with a cracked tooth. Given inputs such as geometry of the tooth and crack, a Finite Element Method (FEM) program is first used to compute individual tooth stiffness. Then, DANST computes meshing stiffness by superimposing the stiffness of teeth according to gear meshing kinematics. Using numerical methods, the gearbox governing equation (8) is then solved for a complete rotation of the gear repeatedly until the initial condition that results in an identical terminal condition is found.

Broken lines in Figure 3 show the meshing stiffness and its corresponding transmission error of a good gearbox calculated by the DANST. Figure 4 shows the same for a gearbox with a crack in tooth 13.

To identify the meshing stiffness from the transmission error of the simulated gearbox, the gearbox model Eq. (8) is formulated into the state space form (2).

$$\dot{x} = F(x,u;\omega) = \begin{bmatrix} x_2 \\ (T_M - C_{s1}(x_2 - x_4) - K_{s1}(x_1 - x_3))/J_M \\ x_4 \\ a_{41} \\ x_6 \\ a_{61} \\ x_7 \\ (-T_L - C_{s2}(x_8 - x_6) - K_{s2}(x_7 - x_5))/J_L \end{bmatrix}$$

$$\begin{aligned} a_{41} &= [T_{f1}(t) - C_{s1}(x_4 - x_2) - K_{s1}(x_3 - x_1) \\ &- C_g(t)(R_{b1}(R_{b1}x_4 - R_{b2}x_6)) - K_g(t)(R_{b1}(R_{b1}x_3 - R_{b2}x_5))]/J_1 \\ a_{61} &= [T_{f2}(t) - C_{s2}(x_6 - x_8) - K_{s2}(x_5 - x_7) \\ &- C_g(t)(R_{b2}(R_{b2}x_6 - R_{b1}x_4)) - K_g(t)(R_{b2}(R_{b2}x_5 - R_{b1}x_3))]/J_2 \\ \hat{s} &= h(x) = R_{b1}x_3 - R_{b2}x_5 \end{aligned} \tag{12}$$

where $x = [\dot{\theta}_M, \ddot{\theta}_M, \dot{\theta}_1, \ddot{\theta}_1, \dot{\theta}_2, \ddot{\theta}_2, \dot{\theta}_L, \ddot{\theta}_L]$, u is the external excitation, and K_g takes the form of (9) or (10) depending on if a tooth crack is suspected (or one can use equation (10) all the time at the expense of higher computational cost in the case of a good gear.)

The sensitivity equations for (12) are then derived so that gradients can be calculated to carry out a search for optimal value of Fourier coefficients. Solid lines in Figures 3 and 4 show the meshing stiffness found by the embedded modeling method for good and cracked gears, respectively. The 5X errors are shown in the bottom of each figure. It is obvious that the meshing stiffness is accurately identified in both cases.

EXPERIMENTAL STUDY

Figure 5 shows the gear test rig. It is consisted of a 40 HP variable speed motor and a 75 HP generator between which a testing gearbox is installed. Transducers are available to measure vibration, input torque, and transmission error with a resolution of $7*10^{-5}$ rad. Additionally, crack gauges and bore scopes are installed to track the evolution of gear faults such as tooth crack and pitting. The 10 HP single-stage spur gearbox used in this study contains a pinion of 23 teeth, and a gear of 54 teeth. The nominal pinion speed is 450rpm and the maximum input torque is 920in-lb. In a test, a small notch was made with wired electrical discharge machining at the root of tooth 17 to create a stress concentration which eventually led to a propagating crack. The transmission errors measured when the tooth is healthy and when it has a crack of 0.18 inches are shown in Figure 6 in solid lines. Notch filtering is then applied to remove the once-per-revolution frequency due to eccentricity.

Figures 7b and 7d show the meshing stiffness identified by the proposed method and their corresponding transmission error in Figures 7a and 7c along with the measured transmission error. When the gear is good, the identified meshing stiffness (7b) is roughly repeated from tooth to tooth as expected. Because of the cracked tooth, the transmission error in Figure 7c has a clear transient around 1,100 along the horizontal axis. This transient becomes even more pronounced in the meshing stiffness. Such increased sensitivity will enable one to detect the crack at an early stage.

CONCLUSIONS

This paper describes the development of an embedded model for a gearbox, which, in turn, enabled the identification of gear meshing stiffness from its vibration. When applied to a simulated gearbox, the method resulted in accurate identification of meshing stiffness which gives an accurate account of the state of gear. When applied to real data taken from a gear test, the meshing stiffness appears to be more sensitive to the crack than the vibration. In addition to increased sensitivity, the ability to identify meshing stiffness makes it possible to determine the physical size of a crack which is needed for severity assessment and residual life prediction.

REFERENCES

1. Dalpiaz, G., Rivola, A. and Rubine, R., 2000, "Effectiveness and Sensitivity of Vibration Processing Techniques for Local Fault Detection in Gears," Mechanical Systems and Signal Processing, 14(3), pp. 387-412.

2. Choy, F. K., Braun, M. J., Polyshchuk, V., Zakrajsek, J. J., Townsend, D. P., and Handschuh, R. F., 1994, "Analytical and Experimental Vibration Analysis of a Faulty Gear System," NASA Technical Memorandum 1.15:106689.

3. Yimin Fan and C. James Li, "Nonlinear System Identification Using Lumped Parameter Models with Embedded Feedforward Neural Networks," Symp. on Sensor-Based Control for Manufacturing, ASME International Mechanical Engineering Congress and Exposition, Anaheim, CA, Nov. 15-20, 1998, Manufacturing Science and Engineering, MED Vol. 8, Editor J. Lee, ASME, New York, 1998, p 579-587.

4. H-H. Lin, R. L. Huston and J. J. Coy, 1988, "On Dynamic Loads in Parallel Shaft Transmissions: Part I-Modeling and Analysis," Journal of Mechanisms, Transmissions, and Automation in Design, Vol. 110, pp. 221-225.

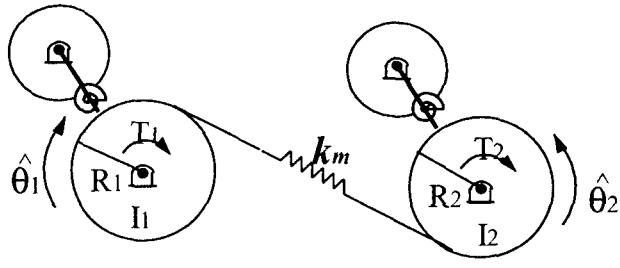

Figure 1. Gear dynamic model

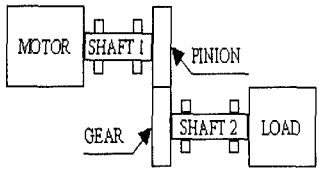

(a)

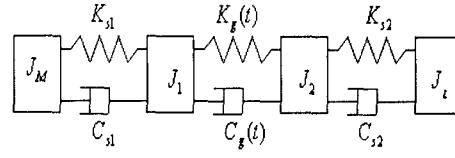

(b)

Figure 2. (a) A spur gear system, (b) A model of the gear system

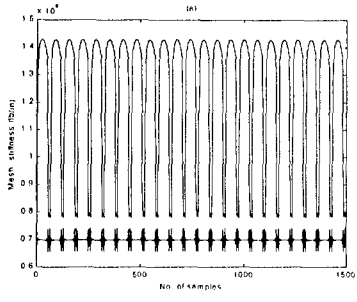

(a) The meshing stiffness $K_g(t)$

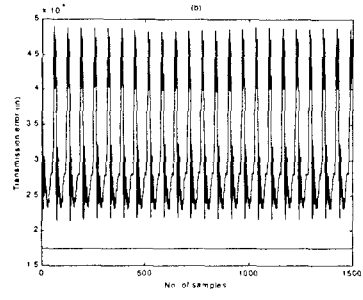

(b) The transmission error.

Figure 3. Meshing stiffness and simulated transmission error of a good gear

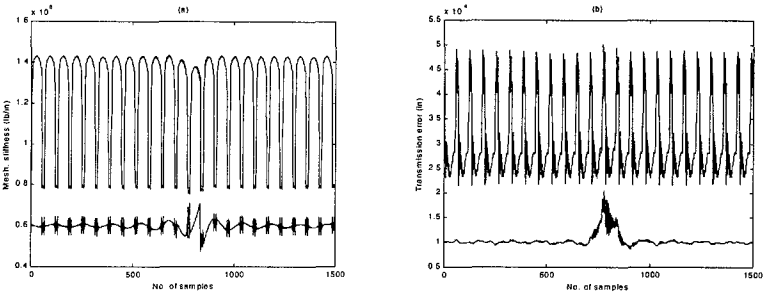

(a) The meshing stiffness $K_g(t)$ (b) The transmission error.

Figure 4. Meshing stiffness and simulated transmission error of a cracked gear

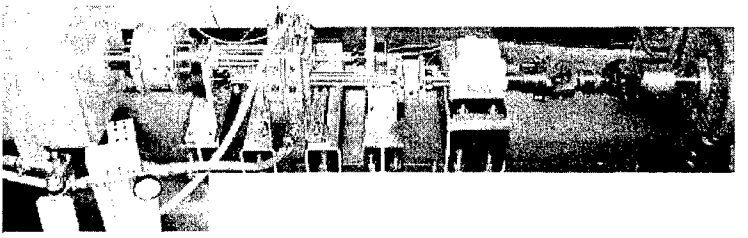

Figure 5. The gear test setup

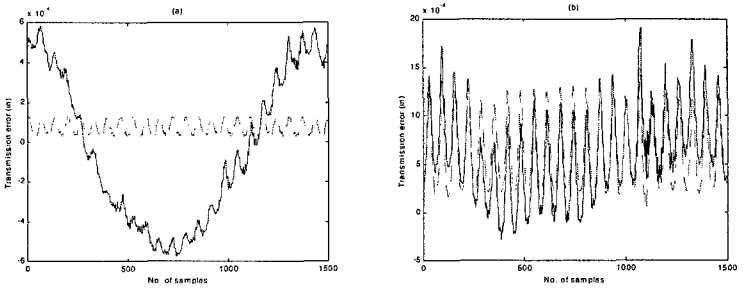

(a) normal gear (b) cracked gear

Figure 6. Transmission error (-measured, --filtered)

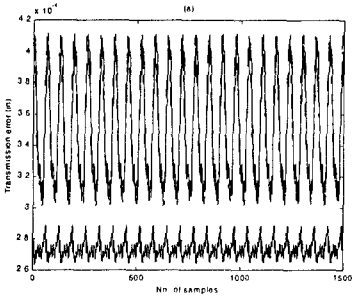

(a) Transmission error (gear is good)

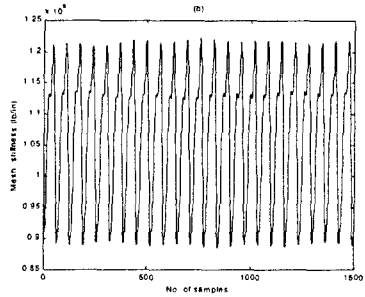

(b) Identified meshing stiffness

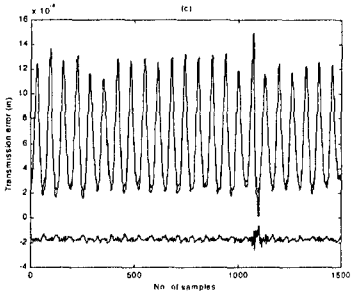

(c) Transmission error (tooth has a .18" crack),

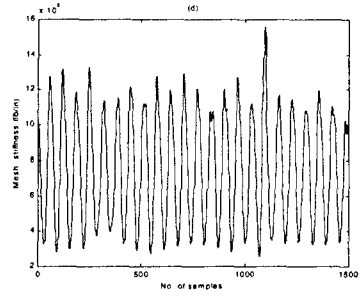

(d) Identified meshing stiffness

Figure 7. Transmission errors and meshing stiffness of the test gear (-experimental, -- identified, 0.5X error)